American Mineralogist, Volume 76, pages 1344–1355, 1991

Evidence for postentrapment diffusion of hydrogen into peak metamorphic fluid inclusions from the massive sulfide deposits at Ducktown, Tennessee

DONALD L. HALL,* ROBERT J. BODNAR, JAMES R. CRAIG
Department of Geological Sciences, Virginia Polytechnic Institute and State University, Blacksburg, Virginia 24061, U.S.A.

ABSTRACT

The Ducktown, Tennessee, mining district contains some of the largest metamorphosed pyrrhotite-pyrite-rich massive sulfide bodies in the Appalachian-Caledonian orogen. The ore bodies attained middle amphibolite grade (525–550 °C, 6–7 kbar) during the Taconic orogeny (~480 Ma). Theoretical calculations of C-O-H-S fluid speciation suggest that H_2O and CO_2 generally comprised 94–100 mol% of the molecular species in the peak metamorphic fluid over the entire range of f_{O_2}-f_{S_2} conditions indicated by silicate + sulfide + oxide ± graphite equilibria in the massive sulfide deposits and country rocks. Other significant species were CH_4 (≤1 mol%) at low f_{O_2}-f_{S_2} and H_2S (≤3 mol%) at low f_{O_2}-high f_{S_2}. The fluid in equilibrium with rocks bearing primary H_2O-CH_4-NaCl fluid inclusions in peak-metamorphic clinopyroxene is calculated to be essentially H_2O-CO_2 with X_{CO_2} = 0.10, which disagrees with observed fluid inclusion compositions. Methane was never a significant component at P-T-f_{O_2}-f_{S_2} conditions indicated by mineral assemblages in the pyroxene-bearing rocks; its presence in primary fluid inclusions suggests a much more reducing environment.

A model for the postentrapment behavior of hypothetical peak metamorphic fluid inclusions and their host rocks indicates that during the initial stages of uplift a modest f_{H_2} gradient between inclusions and grain boundary fluids would have been established if the oxidation state of the latter fluids was buffered by the local mineral assemblage (Py + Po + Mt). A larger f_{H_2} gradient (e.g., 30–15 bars at 550–400 °C) may have been established if fluid infiltrated the ore zones from the relatively reduced country rock (Po-Ilm-graph). It is probable that H diffusion into primary fluid inclusions would have occurred under these conditions. An amount of H approximately equal to 12.5% of the total H originally present in the inclusions must be added to equilibrate f_{H_2} inside peak-metamorphic fluid inclusions with fluid in the surrounding rocks at 450 °C. Diffusive addition of H has profound effects on the P-V-X properties of the trapped fluid. Most importantly, the final composition of the fluid inclusions is X_{H_2O} = 0.90, X_{CO_2} = 0.07, X_{CH_4} = 0.03, and X_{H_2S} = 0.001, which compares favorably with the actual composition estimated from primary fluid inclusions (X_{H_2O} = 0.93, X_{CO_2} = 0.03, X_{CH_4} = 0.04, and X_{H_2S} = 0.001). Our model for H diffusion is consistent with observed δD values of primary fluid inclusions in pyroxene, which are 65‰ too low to have been in equilibrium with local hydrous mineral phases at the temperature of peak metamorphism and can be explained by diffusive addition of isotopically light H to the inclusions.

INTRODUCTION

A study of fluid inclusions from the metamorphosed massive sulfide deposits at Ducktown, Tennessee (Hall et al., 1991) indicates that fluids with a wide range of compositions in the C-O-H-S salt system were involved in the syn- to postmetamorphic history of these deposits. Data from secondary fluid inclusions in quartz combined with various mineralogical, geological, and geochronological constraints allow construction of a P-T-time path that documents early post-Taconic, temperature-concave uplift. The data also suggest that fluctuations in near-isothermal fluid pressure occurred during Alleghanian thrusting in response to episodic fracturing that allowed generation of pressures intermediate between lithostatic and hydrostatic.

Coarse grained (up to 10 cm) clinopyroxene (Di_{55-93}-$Hd_{42-4}Jo_{7-2}$) is uncommon within the ore bodies and generally coexists with amphibole + calcite + quartz + pyrrhotite ± garnet ± pyrite ± magnetite ± anhydrite. The pyroxene invariably contains large (up to several hundred micrometers) primary fluid inclusions containing a low-salinity aqueous liquid, CH_4-rich vapor, and, at room temperature, daughter crystals of quartz, calcite, and in

* Present address: Amoco Production Company, Research Center, P.O. Box 3385, Tulsa, Oklahoma 74102, U.S.A.

0003–004X/91/0708–1344$02.00

some cases pyrrhotite. Similar, apparently primary inclusions are rarely observed in amphibole and garnet coexisting with pyroxene, although these are much smaller (<5 μm) and not suitable for detailed study. Reintegration of all fluid and solid components found in fluid inclusions in pyroxene into a homogeneous fluid, assuming that C in carbonate and S in pyrrhotite were present in the peak metamorphic fluid as CO_2 and H_2S, respectively, results in a normalized volatile composition of 93 mol% H_2O, 4 mol% CH_4, 3 mol% CO_2, and 0.1 mol% H_2S (Hall et al., 1991). In this paper, the volatile composition presented above is compared to calculations of C-O-H-S fluid speciation. A model for H diffusion into primary fluid inclusions is presented to explain the discrepancies between calculated and observed fluid compositions.

Geologic setting

The Ducktown mining district is located in the southeast corner of Tennessee in the Blue Ridge Province of the southern Appalachians (Fig. 1). Eight major ore bodies, ranging in size from 0.25 to 70 million tons (180 million tons total), are contained within the Late Precambrian Copperhill Formation of the Great Smoky Group within the Ocoee Series. The ore bodies vary from massive to disseminated but consist on average of 65 vol% massive sulfide and 35 vol% gangue. The massive sulfide ranges from pyrrhotite rich to pyrite rich but consists in general of 60 vol% pyrrhotite, 30 vol% pyrite, 4 vol% chalcopyrite, 4 vol% sphalerite, and 2 vol% magnetite (Magee, 1968). Other reported metallic phases include galena, molybdenite, tetrahedrite, native bismuth, cubanite, stannite, bornite, rutile, and ilmenite. Traces of Au and Ag have been reported from assays, but the mineralogic hosts for these metals remain unknown, as no discrete phase containing precious metals has ever been reported. Gangue minerals include tremolite, actinolite, cummingtonite, biotite, muscovite, stilpnomelane, chlorite, quartz, calcite, dolomite, rhodochrosite, talc, clinopyroxene, plagioclase, garnet, epidote-group minerals, anhydrite, and rhodonite.

Detailed stratigraphic studies have been conducted by Emmons and Laney (1926), Magee (1968), and Holcombe (1973). The ore bodies are located within one to three stratigraphic horizons but are difficult to correlate because of the effects of deformation. The host rocks are dominantly metagraywackes and quartz-mica schists and minor quartzite, metaconglomerate, and calc-silicate hornfels. The hornfels contains plagioclase, quartz, calcite, clinozoisite, hornblende, garnet, and sphene, occurs as irregular podlike masses within metagraywacke, and may represent metamorphosed calcareous concretions (Hadley and Goldsmith, 1963). In addition, several rock types occur only near the ore bodies, including chlorite schist, muscovite schist, biotite schist, plagioclase-rich rock, and spessartine-rich rock. Similar rock types have been recorded near other metamorphosed massive sulfides (e.g., Gair and Slack, 1984) and have been interpreted to represent either metamorphosed volcaniclastic rocks or metamorphosed equivalents of alteration zones and exhalites typically found around unmetamorphosed volcanogenic massive sulfide deposits (Henry et al., 1979; Gair and Slack, 1984).

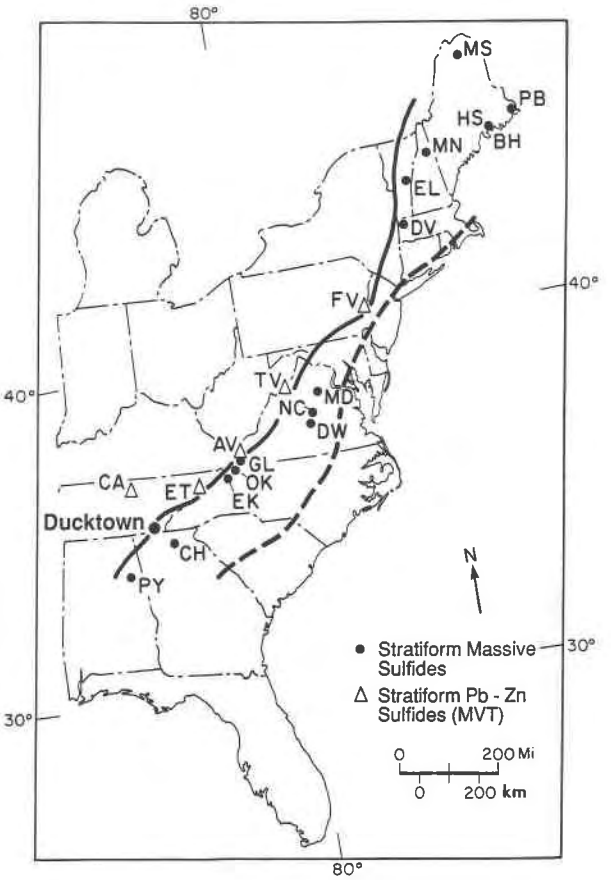

Fig. 1. Index map of the eastern United States showing the locations of stratiform ore deposits in the Appalachians. MS = Machias, PB = Pembroke, HS = Harborside, BH = Blackhawk, MN = Milan, EL = Elizabeth, DV = Davis, FV = Friedensville, TV = Timberville, MD = Mineral District, NC = New Canton, DW = Dillwyn, AV = Austinville, GL = Great Gossan Lead, OK = Ore Knob, EK = Elk Knob, ET = East Tennessee, CA = Carthage, CH = Chestatee, PY = Pyriton. Modified from Craig (1983).

The ore bodies were formed in a rift environment by a sea-floor hydrothermal system associated with the opening of Iapetus in the Late Precambrian (Mauger, 1972; Addy, 1973; Nesbitt, 1979). The deposit was metamorphosed and deformed during the Taconic (~480 Ma) and Alleghanian (~320–270 Ma) orogenies (Holcombe, 1973; Addy and Ypma, 1977). Peak metamorphism, characterized by the assemblage staurolite ± kyanite, occurred at 6–7 kbar and 525–550 °C (Nesbitt and Essene, 1982; Brooker et al., 1987; Hall et al., in preparation). Metamorphism and deformation document compressional tectonics associated with the closing of Iapetus, beginning in the Middle to Late Cambrian and culminating in con-

TABLE 1. Notation

a	empirical coefficient of the RK	m	pertaining to the fluid mixture
a_C	activity of carbon	Mt	magnetite
Act	actinolite	Musc	muscovite
An	anorthite	n_i	initial number of moles
Anhy	anhydrite		
b	empirical coefficient of the RK	n_f	final number of moles
		P_{fluid}	fluid pressure
Cc	calcite	Po	pyrrhotite
Czo	clinozoisite	Py	pyrite
Di	diopside	Qtz	quartz
f	fugacity	R	gas constant
Gt	garnet	Rut	rutile
Graph	graphite	Titan	titanite
i	fluid component	T	temperature
ij	interaction between unlike molecules	Trem	tremolite
		V	mean molar volume
Ilm	ilmenite	X	mole fraction
j	fluid component	Zo	zoisite
Ksp	K-feldspar	γ	fugacity coefficient
		Δ_{a-b}	isotopic fractionation

tinent-continent collision of North America and Africa during the Carboniferous and Permian (Hatcher, 1978).

C-O-H-S FLUID CALCULATIONS

Method

Speciation in the peak metamorphic fluids was calculated using the "equilibrium constant–mass balance" technique (French, 1966; Eugster and Skippen, 1967; Holloway, 1977; Ohmoto and Kerrick, 1977; Ferry and Baumgartner, 1987). The general procedure of Ohmoto and Kerrick (1977) was modified to allow for C activity less than 1 and for nonideal mixing in the fluid phase. In a homogeneous C-O-H-S fluid, five variables must be specified for the system to be invariant. However if graphite is present, then the system is invariant when four parameters are defined. By fixing the fluid pressure (P_{fluid}), temperature (T), oxygen fugacity (f_{O_2}), sulfur fugacity (f_{S_2}), and the activity of C (a_C), the system is completely constrained. We have assumed that the species present are H_2, O_2, S_2, H_2O, H_2S, CO_2, COS, CO, SO_2, and CH_4, which are related through the linearly independent reactions

$$C + O_2 = CO_2 \quad (1)$$

$$CO + \tfrac{1}{2}O_2 = CO_2 \quad (2)$$

$$H_2 + \tfrac{1}{2}O_2 = H_2O \quad (3)$$

$$CH_4 + 2O_2 = CO_2 + 2H_2O \quad (4)$$

$$\tfrac{1}{2}S_2 + O_2 = SO_2 \quad (5)$$

$$CO + \tfrac{1}{2}S_2 = COS \quad (6)$$

$$\tfrac{1}{2}S_2 + H_2O = H_2S + \tfrac{1}{2}O_2 \quad (7)$$

and the constraint that

$$\sum X_i = 1 \quad (8)$$

(see Table 1 for all notation).

Functions describing the equilibrium constants for Reactions 1–7 are presented in Ohmoto and Kerrick (1977). Fugacity coefficients for ideal mixing were taken from Burnham et al. (1969) for H_2O, Burnham and Wall (1974) for CO_2, Shaw and Wones (1964) for H_2 below 3 kbar, and from the reduced variable equations of Ryzhenko and Volkov (1971) for CO, CH_4, SO_2, COS, and H_2S and for H_2 above 3 kbar. Following Ohmoto and Kerrick (1977) γ_{S_2} was assumed to be unity. Fugacities were then calculated from the equation

$$(f_i)_{P_{fluid},T} = X_i\,\gamma_i P_{fluid}. \quad (9)$$

Fugacities for real mixing were calculated from the equation

$$\ln(f_i) = \ln[V/(V - b_m)] + b_i/(V - b_m) - [2\sum X_j a_{ij}/(RT^{1.5}b_m)]\ln[(V + b_m)/V] + (a_m b_i/b_m^2 RT^{1.5})\{\ln[(V + b_m)/V] - b_m/(b_m + V)\} - \ln(V/RT) \quad (10)$$

(Flowers and Helgeson, 1983). The a and b terms were generated from the subroutine MRKMIX (Holloway, 1981). The general Redlich-Kwong equation was then solved explicitly for mean molar volume.

To calculate the mixing terms a and b, the mole fractions of the species must be known. These were obtained by assuming ideal mixing to calculate the initial real mixing fugacity coefficients and then, using the resulting mole fractions as the new mole fractions, to recalculate the real mixing fugacity coefficients. Convergence is reached in about six iterations. The criterion for convergence is that the relative variation in mole fraction between two successive iterations is less than 10^{-4} for all species.

Mineralogical constraints on fluid composition

Major components. The four reactions:

$$Trem + Cc + Qtz = Di + H_2O + CO_2 \quad (11)$$

$$2Zo + CO_2 = Cc + 3An + H_2O \quad (12)$$

$$Musc + Cc + Qtz = Ksp + An + H_2O + CO_2 \quad (13)$$

$$Rut + Cc + Qtz = Titan + CO_2 \quad (14)$$

constraint X_{CO_2} within the ore bodies and country rocks, with the assumption that $X_{H_2O} + X_{CO_2} = 1$. As will be shown, this restriction is generally valid except at conditions of lowest f_{O_2}, highest f_{S_2}, or both indicated by sulfide + oxide + graphite equilibria at Ducktown. Figure 2 shows the projection of these devolatilization reactions onto T-X_{CO_2} space for P_{fluid} = 6 kbar (see Nesbitt, 1979).

A lower limit for X_{CO_2} in the country rocks is provided by Zo(Czo) + An + Cc + Qtz, typically found in nodules of calc-silicate hornfels within metagraywacke. This assemblage restricts X_{CO_2} to approximately 0.10 at peak metamorphic conditions of 550 °C and 6 kbar (Fig. 2); however, in the metagraywackes and schists, which make up the bulk of the country rocks, the assemblage Cc +

An without epidote-group minerals suggests X_{CO_2} greater than 0.10. An + Ksp + Musc + Cc + Qtz is common in the country rocks and restricts X_{CO_2} to about 0.15 at 550 °C (Fig. 2). Assemblages indicative of $0.10 < X_{CO_2} < 0.15$ (e.g., An + Musc + Ksp + Qtz) and $0.15 < X_{CO_2} < 0.85$ (e.g., An + Musc + Cc + Qtz) are also present. Rut + Cc + Qtz is not observed in the country rocks and hence provides an upper limit of approximately 0.35 for X_{CO_2} at 550 °C. No systematic spatial variations in the major fluid components H_2O and CO_2 were observed, as assemblages indicating relatively high X_{CO_2} can be found a few meters from those indicating low X_{CO_2}. It appears that fluid composition was largely controlled by the local metamorphic mineral assemblage and that X_{CO_2} varied between >0.10 and <0.35 within the country rocks.

In the ore zones, Di-Trem-Cc-Qtz restricts X_{CO_2} to approximately 0.10 at 550 °C. In some samples, clinozoisite or zoisite and plagioclase coexist with the above assemblage, a further indication of an X_{CO_2} near 0.10 (Fig. 2). In some rocks, amphibole is clearly retrograde, plagioclase is missing, and the stable peak metamorphic assemblage appears to have been Di + Cc + Qtz; thus, X_{CO_2} varied to less than 0.10. In most of the calc-silicate rocks, the stable mineral assemblage is Trem + Cc + Qtz, implying $X_{CO_2} > 0.10$. As in country rocks, samples from the ore zones contain mineral assemblages indicative of X_{CO_2} conditions on either side of Equilibrium 13. In addition, Rut + Cc + Qtz is not uncommon, suggesting X_{CO_2} in excess of 0.35. To summarize, X_{CO_2} conditions in the ore zones appear to have varied from values less than 0.1 to values somewhat greater than 0.35. As in the country rocks, there is no discernible trend in fluid composition in the ore zones, and fluid composition appears to have been locally controlled. This is consistent with centimeter-scale variations in oxide + sulfide mineral assemblages that indicate small-scale variations in f_{O_2} and f_{S_2} (see below). Relatively high X_{H_2O} conditions indicated by mineral assemblages in pyroxene-bearing samples are consistent with compositions of primary fluid inclusions found in pyroxene ($X_{H_2O} \approx 0.9$–0.95); however, as will be shown, we believe that the original compositions of these inclusions have been modified to slightly higher X_{H_2O}.

The addition of salt to fluid-mineral systems depresses the stability fields of mineral assemblages on the CO_2-bearing sides of Reactions 11–14 by increasing the activity of CO_2 in the fluid phase (Jacobs and Kerrick, 1981; Bowers and Helgeson, 1983). Thus, the maximum and minimum X_{CO_2} conditions actually experienced by rocks at Ducktown may be significantly less than estimated above. The presence of appreciable amounts of dissolved constituents in peak metamorphic fluids is indicated by primary fluid inclusions in pyroxene, which contain 3 wt% NaCl equivalent and imply over 11 wt% total dissolved solids in the trapped fluid (Hall et al., 1991).

Estimates of f_{O_2} and f_{S_2}. Conditions of f_{O_2} and f_{S_2} are reasonably well constrained by silicate + oxide + sulfide + graphite equilibria at Ducktown. By considering equilibria among mineral assemblages bearing Fe-Ti-Ca-C-O-S, Nesbitt and Kelly (1980) concluded that f_{O_2} and f_{S_2} generally increase as the ore bodies are approached. They suggested minimum values of log f_{O_2} of −22.0 and log f_{S_2} of −6.5 for the country rocks and maximum values of log f_{O_2} of −18.3 and log f_{S_2} of −2.7 for Py + Po + Mt ore. Relevant phase equilibria in the system Fe-Ti-O-S are shown in Figure 3. Our microprobe analyses of sulfide and oxide phases indicate that pyrite, rutile, and magnetite are virtually pure end-members, whereas il-

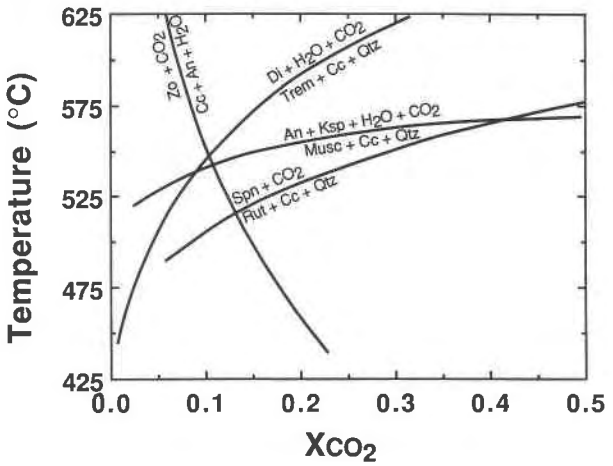

Fig. 2. T-X_{CO_2} relations calculated for P_{fluid} of 6 kbar, illustrating X_{CO_2}-constraining equilibria pertinent to mineral assemblages at Ducktown. Modified after Nesbitt (1979). Original experimental data from Johannes and Orville (1972), Hewitt (1973), Slaughter et al. (1975), and Hunt and Kerrick (1977).

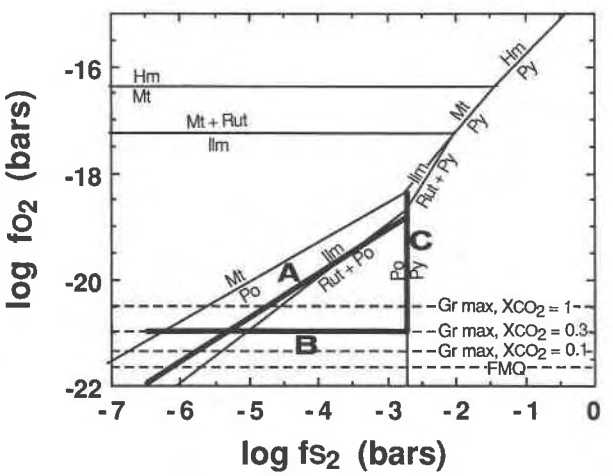

Fig. 3. Relations of f_{O_2}-f_{S_2} in the system Fe-Ti-O-S at 6 kbar and 550 °C. Also shown is the f_{O_2} of the graphite maximum calculated from Equation 1, assuming maximum X_{CO_2} of 1.0, 0.3, and 0.1. The f_{O_2} of FMQ is shown for reference. A, B, and C refer to f_{O_2}-f_{S_2} trends used to model fluid composition, where A is the trend suggested by Nesbitt and Kelly (1980). Data from Toulmin and Barton (1964), Robie et al. (1978), and Barton and Skinner (1979).

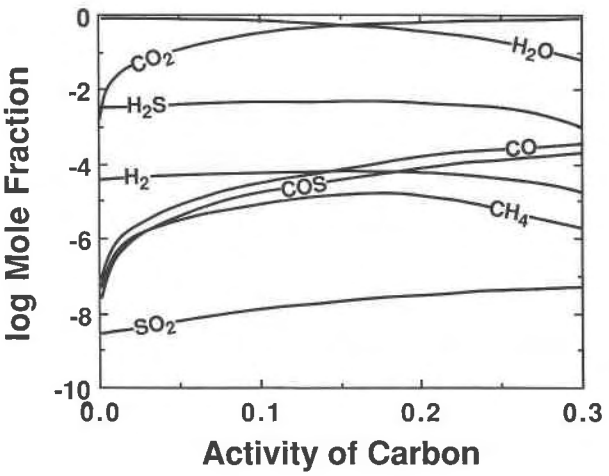

Fig. 4. Log X_i-a_C diagram calculated for 6 kbar, 550 °C, log $f_{O_2} = -20$, and log $f_{S_2} = -3$, showing the variation in fluid composition with the activity of C. In this and all subsequent diagrams the activity of C is defined as $a_C = 1$ for graphite.

menite contains an average of 2 mol% Fe_2O_3, 1 mol% MgO, and 1 mol% MnO. Pyrrhotite contains an average of 47.5 at.% Fe. The effects of solid solution have been ignored in constructing Figure 3.

Away from the ore bodies, within staurolite grade country rocks, the common sulfide + oxide + graphite assemblage is pyrrhotite + ilmenite + graphite; however, pyrrhotite + pyrite + ilmenite was also noted. As the ore bodies are approached, primary graphite disappears and rutile replaces ilmenite as the stable Ti-oxide phase. Within the ore bodies themselves, the common assemblages are Po ± Py ± Mt ± Rut. However, other apparently stable assemblages were noted, including Po + Rut + Graph, Po + Py + Graph, Po + Py + Rut + Graph, and Po + Py + Mt + Ilm. These assemblages, although not significantly extending the range of f_{O_2} or f_{S_2} delineated by Nesbitt and Kelly (1980), do suggest that in many cases no smooth trend of increasing f_{S_2} and f_{O_2} exists as the ore bodies are approached. Specifically, it appears that f_{O_2} remained low in much of the country rock and wallrock and attained values approaching pyrrhotite-pyrite-magnetite only in certain portions of the ore bodies. The presence of native bismuth in galena and the rare occurrence of primary graphite with calcite indicate low f_{O_2} conditions in these portions of the ore zones. A similar conclusion was reached by Nesbitt (1982) while investigating sulfide + silicate equilibria. He found that, in general, the X_{Fe} of biotite, garnet, staurolite, and chlorite decreased toward the ore and that the distribution and composition of these phases were consistent with a progressive increase in f_{S_2} toward the ore, but that a decrease in f_{O_2} was required within the wallrocks and ore zones.

The foregoing indicates that f_{O_2} and f_{S_2} were variable within ore zones and country rocks. This is consistent with our T-X_{CO_2} analysis, which suggests that fluid composition was largely controlled by local lithologies.

Activity of C. In the country rocks, where graphite is common, the activity of C is defined to be unity. The general absence of primary graphite in the ore bodies and wallrock implies reduced a_C, consistent with the location of the graphite maximum at log f_{O_2} of −20.5, as calculated from Reaction 1 at 6 kbar and 550 °C (Fig. 3). At the graphite maximum, the fluid is essentially pure CO_2; however, mineral assemblages in the country rocks fix maximum X_{CO_2} near 0.3. Therefore, a better estimate of the graphite maximum is obtained by setting X_{CO_2} equal to 0.3 and calculating f_{O_2} from Reaction 1, which results in an estimated log $f_{O_2} = -21.0$ (Fig. 3). At f_{O_2} conditions above that of the estimated graphite maximum, fluid composition is dependent on the activity of C. Figure 4 shows fluid composition as a function of a_C at 6 kbar, 550 °C, log $f_{O_2} = -20.0$, and log $f_{S_2} = -3.0$. X_{CO_2} increases as a_C increases at constant f_{O_2}, and depending on the activity of C at any f_{O_2} above the graphite maximum, the fluid composition varies from virtually pure H_2O to pure CO_2 at P-T-f_{S_2} conditions considered here (Fig. 4).

Within the ore zones, the most oxidized mineral assemblages (i.e., those containing Py + Po + Mt) invariably indicate the lowest X_{CO_2} conditions (≤ 0.10). When graphite is found with low X_{CO_2} assemblages, it is always secondary (i.e., precipitated by retrograde fluids). Primary graphite, present during peak metamorphism, does occur rarely in the ore zones, but the accompanying silicate + oxide + sulfide assemblages are consistent with relatively low f_{O_2}, high X_{CO_2} conditions ($0.1 < X_{CO_2} < 0.4$). As previously mentioned, there is no systematic trend in X_{CO_2} in the wallrocks or ore zones. Because the ranges of X_{CO_2} recorded in the country rocks and ore zones are similar, we have arbitrarily chosen to model the activity of C along the f_{O_2}-f_{S_2} trend of Nesbitt and Kelly (1980) by (1) assuming it is constant above the graphite maximum for $X_{CO_2} = 0.3$ (log $f_{O_2} = -21.0$) and is equal to 0.001, thereby producing a fluid with $X_{CO_2} = 0.10$ at the f_{O_2}-f_{S_2} conditions indicated by Py + Po + Mt and (2) assuming it varies above the graphite maximum for $X_{CO_2} = 0.1$ (log $f_{O_2} = -21.4$) in order to maintain an X_{CO_2} of 0.1. The latter requires that a_C decreases fairly regularly from 1 at log f_{O_2} of −21.4 to 0.001 at Py + Po + Mt. Considering the nonsystematic local control of fluid composition within the country rocks and ore zones, it is improbable that a_C varied smoothly from country rock to ore zones but rather oscillated in response to the same local controls of fluid composition.

Results

Fluid speciation was calculated for points along the suggested f_{O_2}-f_{S_2} trend of Nesbitt and Kelly (1980) with a_C modeled as described above (Fig. 5). Results indicate that H_2O and CO_2 were generally the dominant molecular species, comprising 94–100 mol% of the peak metamorphic fluid. At the low f_{O_2}-f_{S_2} end of the trend, CH_4 reaches 1 mol%, but the lower limit of f_{O_2} is not well constrained by the oxide + sulfide mineral assemblages, and significantly larger proportions of CH_4 are possible at lower f_{O_2}

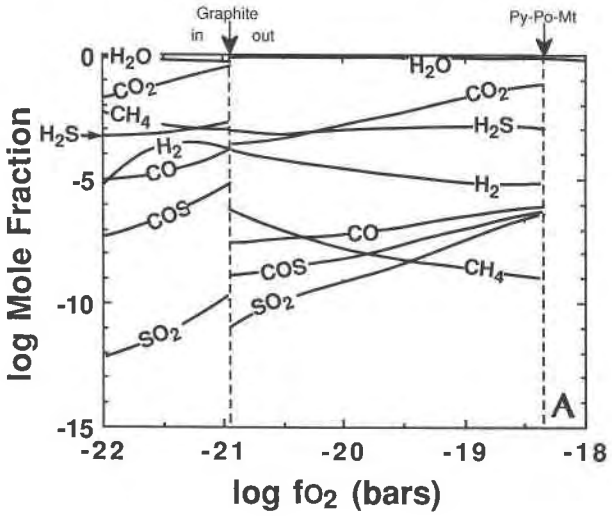

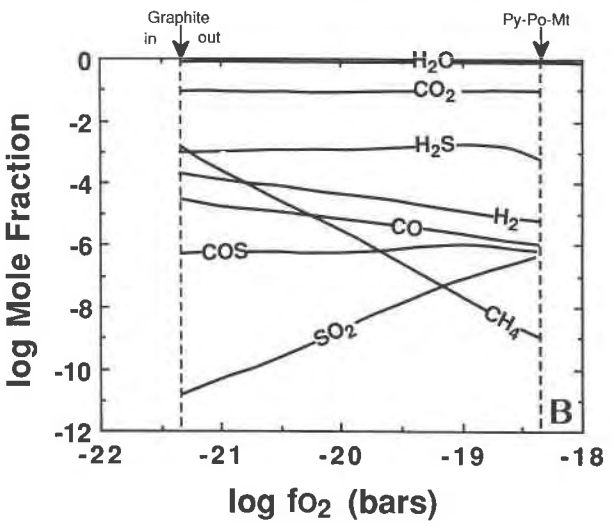

Fig. 5. X_i-f_{O_2} relations calculated for 6 kbar and 550 °C with f_{O_2} and f_{S_2} constrained by trend A (Fig. 3). (**A**) The $a_C = 0.001$ above log f_{O_2} of −20.96, which produces a maximum X_{CO_2} of 0.3. (**B**) $X_{CO_2} = 0.10$ ($a_C = 1 - 0.001$). The graphite maximum is located at $f_{O_2} = -21.35$, which corresponds to a X_{CO_2} of 0.1.

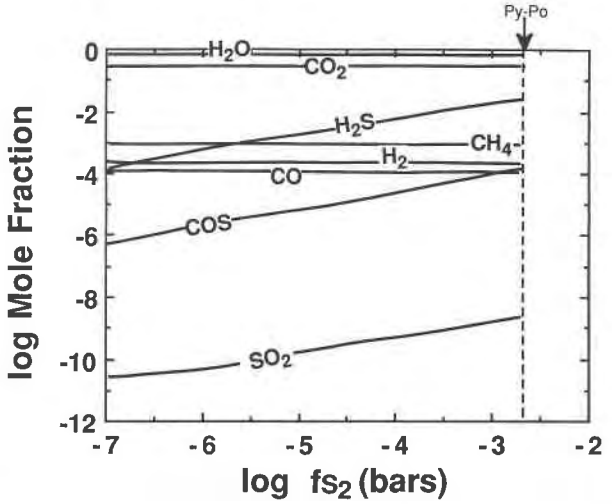

Fig. 6. X_i-f_{S_2} relations calculated for 6 kbar and 550 °C with f_{O_2} constant at −20.96 (trend B, Fig. 3). An f_{O_2} of −20.96 corresponds to an X_{CO_2} of 0.3.

(e.g., 7 mol% CH_4 at log $f_{O_2} = -23.0$, log $f_{S_2} = -6.5$). However, if X_{CO_2} were ≥0.1 everywhere, as suggested by silicate mineral assemblages, the minimum log f_{O_2} would be −21.4 and the maximum X_{CH_4} would be less than 1 mol%. Above the graphite maximum, H_2O and CO_2 dominate, and the ratio of these two species is completely dependent on the value chosen for a_C. If a_C is constant at 0.001 (Fig. 5A), then the fluid varies from pure H_2O just above the graphite maximum to H_2O + CO_2 with X_{CO_2} = 0.1 at the Po-Py-Mt buffer. At higher f_{O_2}-f_{S_2} conditions, X_{H_2O}, X_{CH_4}, and X_{H_2} decrease; X_{CO_2}, X_{CO}, X_{SO_2}, and X_{COS} increase; and X_{H_2S} remains relatively constant (Fig. 5A). If X_{CO_2} is constant at 0.1 along the same trend (i.e., model 2 for a_C), X_{H_2O}, X_{CO_2}, X_{H_2S}, and X_{COS} remain approximately constant; X_{CH_4}, X_{CO}, and X_{H_2} decrease; and X_{SO_2} increases (Fig. 5B). While fluid composition is reasonably well constrained at both ends of trend A (Fig. 3), it is poorly constrained in the middle because of uncertainties associated with a_C. Nevertheless, the calculations do imply that the peak metamorphic fluid was essentially a binary H_2O-CO_2 mixture above the graphite maximum, along the f_{O_2}-f_{S_2} trend of Nesbitt and Kelly (1980).

As previously mentioned, mineral assemblages suggest that in some areas f_{O_2}-f_{S_2} conditions deviated significantly from trend A; specifically, low f_{O_2}–high f_{S_2} conditions prevailed in some rocks (trend B, Fig. 3). The apparent equilibrium assemblage Po + Py + Graph ± Titan is observed infrequently within the wallrocks, constraining log f_{S_2} to be −2.7 and log f_{O_2} to be as low as −22 (Fig. 3). At these conditions, the metamorphic fluid is composed of approximately 90 mol% H_2O, 7 mol% H_2S, 2.5 mol% CO_2, and 0.5 mol% CH_4. Fluid composition was calculated assuming constant log $f_{O_2} = -21.0$ ($X_{CO_2} \sim 0.3$) and variable log f_{S_2} between −6.5 and −2.7 (trend B, Fig. 3). Results, presented in Figure 6, indicate that as f_{S_2} increases, CH_4 is replaced by H_2S as the third most abundant species, but that everywhere along trend B X_{CO_2} + $X_{H_2O} \geq 0.97$. As expected, mole fractions of all S species increase as f_{S_2} increases. Mole fractions of other species do not change appreciably.

Many mineral assemblages imply buffering of f_{S_2} by Py + Po at log f_{O_2} conditions between −21.0 (assuming a maximum X_{CO_2} of 0.3 and $a_C = 1$) and −18.3 (Py + Po + Mt). As mentioned above, mineral assemblages in ore zones indicating the lowest f_{O_2} also imply the highest X_{CO_2}. Fluid compositions calculated along this trend (C in Fig. 3) are presented in Figure 7 and assume a linear decrease in X_{CO_2} from 0.3 at log $f_{O_2} = -21.0$ to 0.1 at log $f_{O_2} = -18.3$. H_2S may have comprised up to 3 mol% of the

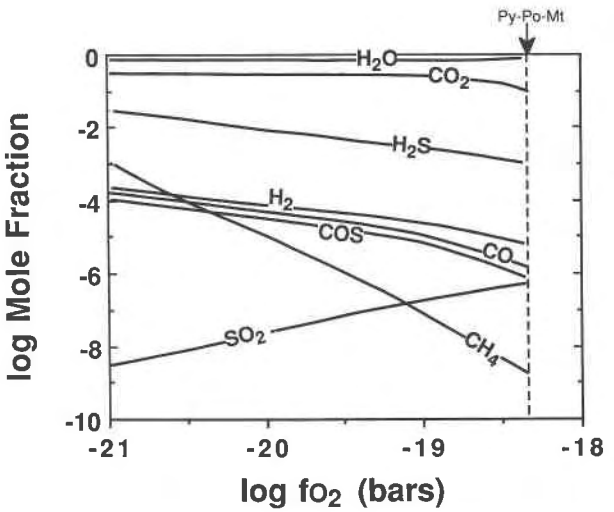

Fig. 7. X_i-f_{O_2} relations calculated for 6 kbar and 550 °C with f_{S_2} constant at −2.7 (trend C, Fig. 3). An f_{S_2} of −2.7 corresponds to the Py-Po equilibrium boundary.

fluid at low f_{O_2}; X_{H_2O} increases and mole fractions of all other species decrease as log f_{O_2} increases (Fig. 7).

Comparison of calculated fluid compositions with primary fluid inclusions

Comparison of calculated peak metamorphic fluid compositions, constrained by mineral assemblages coexisting with clinopyroxene, with the estimated compositions of primary fluid inclusions in clinopyroxene indicates significant similarities and differences (Table 2). Both compositions imply that H_2O was the dominant molecular fluid species during peak metamorphism and that CO_2 was a significant species as well. Also, both predict comparable quantities of H_2S. However, the calculated composition suggests that CH_4 was present in negligible amounts, whereas observed compositions of primary fluid inclusions show that CH_4 is present in proportions subequal to or greater than CO_2. To reconcile the calculated-speciation with fluid-inclusion data would require extremely reducing conditions during trapping, specifically, log f_{O_2} of ~ -22.8 and log f_{S_2} of $\lesssim -6.5$; in other words, conditions within the stability fields of Po + Ilm + Graph or Po + Rut + Graph (Fig. 3) are required. This is inconsistent with the equilibrium mineral assemblages coexisting with pyroxene containing primary fluid inclusions that indicate trapping at log f_{O_2} near −18.3 and log f_{S_2} near −2.7 (i.e., defined by Py + Po + Mt). The discrepancy cannot be explained by any reasonable errors in the determination of P-T-f_{O_2}-f_{S_2}-a_C conditions attending pyroxene growth. Furthermore, reasonable errors in the thermodynamic data used to calculate X_{CH_4} cannot account for the inconsistency. Specifically, varying all fugacity coefficients involved in Reaction 14 by 20% in a direction to maximize X_{CH_4} increases X_{CH_4} by less than half an order of magnitude. A 100% error in all fugacity coefficients or an error in log K for Reaction 4 of 7 orders of magnitude is required to bring observed and calculated methane concentrations into agreement.

TABLE 2. Observed and calculated fluid compositions

Observed	Calculated
$X_{H_2O} = 0.93$	$X_{H_2O} = 0.90$
$X_{CH_4} = 0.04$	$X_{CH_4} = 10^{-9}$
$X_{CO_2} = 0.03$	$X_{CO_2} = 0.10$
$X_{H_2S} = 0.001$	$X_{H_2S} = 0.001$

Pyrrhotite daughters occur in only ~20% of the inclusions studied. They are generally confined to larger inclusions, which suggests that pyrrhotite may be metastably absent from the smaller inclusions. There is no measurable difference in the proportions of major fluid components (e.g., CH_4) between pyrrhotite-bearing and pyrrhotite-absent inclusions, suggesting that elevated CH_4 contents cannot be ascribed to the tendency for pyrrhotite to maintain reducing conditions within the inclusions.

Postentrapment changes in fluid composition

Closed system

A mechanism that could account for the disparity between calculated and observed fluid compositions is continued reequilibration of the trapped molecular species in C-O-H-S fluid inclusions during cooling, resulting in a speciation that is substantially different at room temperature than at the conditions of trapping. The change in speciation during cooling of a hypothetical C-O-H-S fluid inclusion can be calculated using methods outlined by Holloway (1981) and Dubessy (1984).

In this procedure, an inclusion is assumed to contain a fluid of known composition and molar volume at some initial P-T condition (e.g., of trapping or observation). By specifying an arbitrary inclusion volume at this pressure and temperature and assuming the system remains at constant volume, or by correcting for thermal expansion and compressibility of the host mineral, the new composition, molar volume, and internal pressure of the fluid inclusion can be calculated at a specified temperature. The solution requires the functions describing equilibrium constants for Reactions 2–7 (compiled by Ohmoto and Kerrick, 1977), Equation 8, and the additional mass balance equations

$$\sum n_i\mathrm{C} = \sum n_f\mathrm{C} \quad (15)$$

$$\sum n_i\mathrm{O} = \sum n_f\mathrm{O} \quad (16)$$

$$\sum n_i\mathrm{H} = \sum n_f\mathrm{H} \quad (17)$$

$$\sum n_i\mathrm{S} = \sum n_f\mathrm{S}. \quad (18)$$

Fugacity coefficients for the ten species considered are computed from Holloway's (1981) program MRKMIX, and the new P-V-X properties of the inclusion are calculated by simultaneously solving the ten equations (six describing fluid speciation and four describing mass balance) using Newton's method for nonlinear equations

(Burden and Faires, 1985). The criterion for convergence is the same as for our previous calculations.

Closed system speciation changes that result when the calculated peak metamorphic fluid is trapped and cooled to 400 °C are shown in Figure 8. A minimum temperature of 400 °C was chosen for several reasons. Holloway's modified Redlich-Kwong equation of state is only applicable above 400 °C for aqueous fluids. Furthermore, the kinetics of exchange among carbonic fluid species and graphite are very sluggish below 400 °C (Sackett and Chung, 1979; Harting and Maass, 1980; Ziegenbein and Johannes, 1980). Finally, the positions of the solvi of C-O-H-S fluids are unknown but, in general, probably lie at temperatures below the critical point of H_2O. Thus, a minimum temperature of 400 °C restricts calculations to the single fluid phase region.

The major components of the peak metamorphic fluid, namely H_2O and CO_2, vary insignificantly during cooling, but the minor species O_2, S_2, H_2, SO_2, and CH_4 vary up to several orders of magnitude (Fig. 8). This agrees with the conclusion of Dubessy (1984) that it is not possible to render a major fluid component minor or vice versa in the absence of a daughter precipitate, such as graphite, or a mechanism that preferentially removes one or more fluid components. The fluid was assumed to remain undersaturated with respect to graphite during cooling because graphite was not detected petrographically or during Raman analyses. If graphite were to precipitate in the fluid inclusions during cooling, then significant CH_4 may be produced at low temperatures and pressures. Although X_{CH_4} does increase significantly during cooling, the initial quantity of this species is so small (10^{-7} mol%) that an increase of several orders of magnitude leaves CH_4 below detection by any microthermometric or spectroscopic technique.

We conclude that postentrapment compositional changes in a fluid inclusion that remains a closed system cannot explain the disparity between the calculated peak metamorphic fluid composition and the observed composition of primary peak metamorphic fluid inclusions at Ducktown.

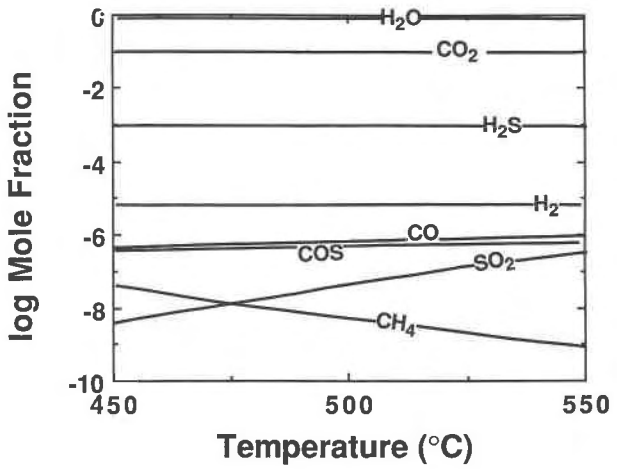

Fig. 8. X_i-T relations showing closed system speciation changes obtained by trapping a peak metamorphic fluid at 6 kbar, 550 °C, log $f_{O_2} = -18.3$, log $f_{S_2} = -2.7$, and $a_C = 0.001$ and cooling it at constant volume to 400 °C.

H diffusion

Several phenomena reported in the fluid inclusion literature have been attributed to the effects of diffusion. Daughter minerals such as hematite, anhydrite, and chalcopyrite, which do not dissolve upon heating, may have precipitated in response to changes in oxidation state or pH resulting from diffusive loss of H (Roedder and Skinner, 1968; Roedder, 1981). Tiny, ubiquitous fluid inclusions in quartz from high grade metamorphic rocks may form by diffusive exsolution of H_2O from the quartz structure during cooling and decompression (White, 1973; Wilkins and Barkas, 1978); H_2O precipitation and diffusion in wet quartz and berlinite ($AlPO_4$) during annealing has been documented (Cordier et al., 1988). Similarly, Sterner et al. (1988) and Hall et al. (1989a) have shown that preferential loss of H_2O from NaCl-KCl-H_2O fluid inclusions in quartz can occur in response to differential pressure between inclusion and matrix. Pasteris and Wanamaker (1988) were able to diffuse O into and out of CO_2-rich inclusions in olivine at 1000–1400 °C, and Hall et al. (1989b) have documented H gain by CO_2-H_2O fluid inclusions in quartz and reduction of CO_2 to CH_4 + H_2O at temperatures as low as 650 °C. Diffusive loss of H_2O from C-O-H inclusions has been suggested as a possible explanation for nearly pure CO_2 inclusions in granulites and other high-grade rocks (Roedder, 1981), and diffusive gain of H and reduction of CO_2 may explain the occurrence of appreciable CH_4 in fluid inclusions from some granulites (Hall and Bodnar, 1989).

The driving force for H diffusion out of or into a fluid inclusion is the f_{H_2} gradient between the host (or that imposed by the fluid circulating through the rock) and the fluid inside the inclusion. These gradients may become appreciable during cooling and decompression. Diffusion rates of H through minerals are sufficiently rapid above 600 °C (Kats, 1962; Kats et al., 1962; Kronenberg et al., 1986) that over geologic time appreciable gradients in f_{H_2} could not be maintained. It is unclear however what the effective blocking temperature is for H diffusion over geologic time. The extent or importance of H diffusion depends on the P-T-time path as well as the compositions of the inclusion and matrix fluid and crystal chemistry.

We have calculated the changes in the f_{H_2} in the matrix fluid and in model peak-metamorphic fluid inclusions during uplift. The inclusions trapped the fluid composition calculated for 6 kbar, 550 °C, log $f_{O_2} = -18.3$, log $f_{S_2} = -2.7$, and $a_C = 0.001$ (Table 2). The uplift path chosen for the matrix was constrained by paragenetic and microthermometric data from secondary fluid inclusions in quartz (Hall et al., 1991) and is slightly concave toward the temperature axis (Fig. 9) over the temperature range

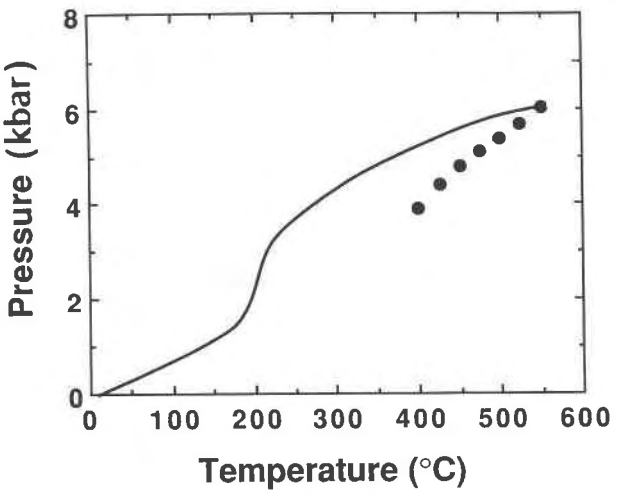

Fig. 9. *P-T* diagram illustrating the uplift path delineated by Hall et al. (1991) for Ducktown rocks (line) and the calculated *P-T* path (pseudoisochore) traversed by hypothetical peak metamorphic fluid inclusions during cooling (dots).

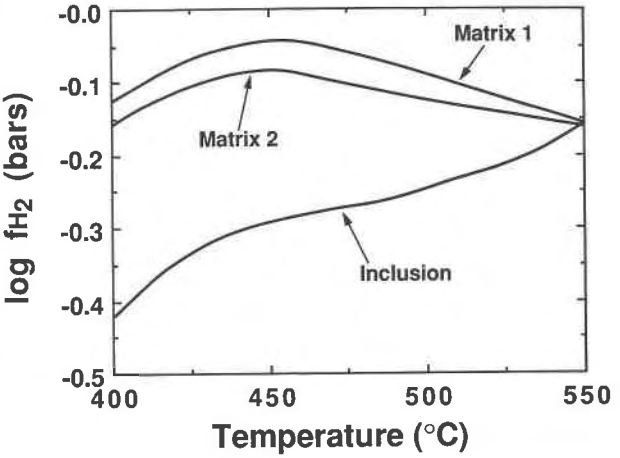

Fig. 10. Relationships for f_{H_2}-T calculated for matrix fluids and a hypothetical peak metamorphic fluid inclusion trapped at 6 kbar, 550 °C, log $f_{O_2} = -18.3$, log $f_{S_2} = -2.7$, and $a_C = 0.001$. Pressures in the matrix during uplift were constrained by Figure 9, and f_{O_2}-f_{S_2} conditions are buffered at Py + Po + Mt. The internal pressure of the fluid inclusion is dictated by the *P-V-T-X* properties of the trapped fluid and the assumption that the inclusion maintains a constant volume. Matrix 1 was calculated assuming a_C is constant and equal to 0.001, and matrix 2 assumes that X_{CO_2} is constant and equal to 0.10.

considered here (550–400 °C). The pseudoisochore calculated by cooling the peak metamorphic fluid at constant volume, but taking into account *P-V-T* variations due to speciation changes, indicates that the hypothetical inclusions are underpressured (i.e., $P_{ext} > P_{int}$) during uplift (Fig. 9). At 400 °C, the pressure differential is about 750 bars. It is significant that many primary fluid inclusions in pyroxene from Ducktown exhibit textures resembling implosion halos produced in synthetic fluid inclusions by Sterner and Bodnar (1989) during laboratory experiments where confining pressures exceeded internal pressures of the fluid inclusions (Hall et al., 1991).

The f_{H_2} gradient established during the postmetamorphic history is presented in Figure 10. For these calculations it is assumed that the matrix fluid composition (i.e., f_{O_2} and f_{S_2}) is buffered by Py-Po-Mt. Two f_{H_2}-T curves were calculated for the matrix, one with a_C constant at 0.001 (matrix 1; Fig. 10) and the other with a_C varying from 0.001 at 6 kbar and 550 °C to 0.159 at 5 kbar and 400 °C, so that X_{CO_2} is constant at 0.10 (matrix 2; Fig. 10). These calculations indicate that f_{H_2} in the matrix is greater than that in the fluid inclusion; in fact, it is four times that in the inclusion at 450 °C, although both fugacities are low and the gradient is only approximately 0.3 bars (Fig. 10). Thus, a small f_{H_2} gradient may have been established during uplift, and this gradient theoretically could have promoted H diffusion into primary fluid inclusions.

The difference in f_{H_2} between matrix and inclusion is magnified by an order of magnitude if the fluid in "H communication" with primary fluid inclusions is not controlled by Py + Po + Mt but by a more reduced assemblage, such as Po + Ilm + Graph or FMQ. This may have occurred if fluid in equilibrium with the bulk of the host metagraywackes and quartz-mica schists, or reduced portions of ore zones, infiltrated high f_{O_2} (pyroxene-bearing) portions of the ore bodies after peak metamorphism. The f_{H_2} gradient resulting from infiltration of a fluid with f_{O_2} buffered by FMQ and f_{S_2} buffered by pyrrhotite with $X_{FeS} = 0.95$, relative to FeS-S_2, is shown in Figure 11. If this fluid comes into diffusive communication with primary fluid inclusions, a f_{H_2} gradient of 15–30 bars will result, again promoting H diffusion into primary fluid inclusions. Secondary fluid inclusions in quartz document influx of post-peak metamorphic fluids into ore zones from external sources; at least one such fluid was responsible for precipitation of secondary graphite and replacement of sulfides by graphite in ore zones. The observed replacement of magnetite and pyrite by pyrrhotite may be evidence for influx of low-f_{O_2}, low-f_{S_2} fluids as well. The ore bodies are relatively small geochemical anomalies contained within a large volume of relatively reduced metasedimentary rocks. As such, it is expected that the ore bodies were exposed to low-f_{O_2}-f_{S_2} fluids after metamorphism. Given the rapid rate of H diffusion through minerals (e.g., Kronenberg et al., 1986), the calculated f_{H_2} gradient between inclusions and externally derived grain boundary fluids could induce addition of H to fluid inclusions in a geologically short time.

We have calculated the amount of H diffusion necessary to eliminate the f_{H_2} gradient between inclusions and matrix at 450 °C. If the matrix fluid is buffered by Py + Po + Mt, diffusion of much less than 0.1 mol% of the total H originally present in the inclusion will negate the f_{H_2} gradient. If the matrix fluid is buffered by FMQ, how-

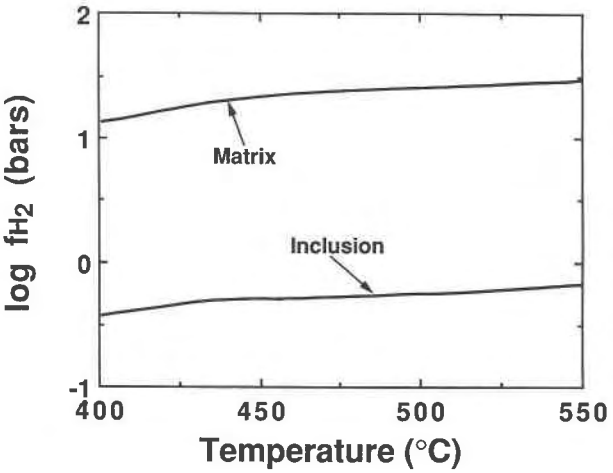

Fig. 11. Relationships for f_{H_2}-T calculated for matrix fluids and a hypothetical peak metamorphic fluid inclusion. Conditions are the same for the inclusion as in Figure 10. Here, the f_{O_2} of the matrix fluid is buffered by FMQ and f_{S_2} is buffered by Po with $X_{FeS} = 0.95$.

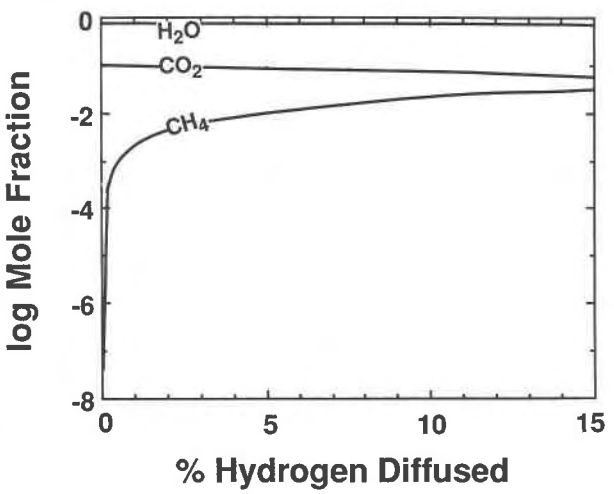

Fig. 12. Variation in X_{H_2O}, X_{CO_2}, and X_{CH_4} during H diffusion at 450 °C. The percent of H diffused is referenced to the total amount of H originally contained within the inclusion prior to diffusion; in other words, it represents the amounts contributed from H_2O, CH_4, H_2, and H_2S.

ever, an amount of H approximately equivalent to 12.5 mol% of the H originally present in the inclusion must diffuse into the fluid inclusion to equilibrate f_{H_2}. Diffusion of this much H into a fluid inclusion has significant effects on the P-V-X properties. The mole fraction of methane increases over 7 orders of magnitude from 10^{-9} to 0.03; the fluid is essentially 90 mol% H_2O, 7 mol% CO_2, and 3 mol% CH_4 after diffusion of 12.5 mol% H (Fig. 12). Methane becomes an important component, which may be detectable during routine microthermometric studies and spectroscopically. Furthermore, the above fluid composition compares favorably with the actual composition estimated for primary fluid inclusions (Table 2).

After diffusion of 12.5% H, the molar volume of the fluid has decreased from 22.8 to 21.6 cm^3 and the internal pressure has increased from 4.8 to 6.4 kbar. Because the matrix is at about 5.5 kbar at 450 °C (Fig. 9), H diffusion results in approximately 900 bars of internal overpressure inside the inclusions, which may be enough to cause the inclusions to stretch (Sterner and Bodnar, 1989). Variable liquid-vapor ratios have been observed in primary fluid inclusions in pyroxene, and clathrate-dissociation temperatures suggest a range of internal pressures at room temperature, perhaps resulting from equilibration toward lower densities during uplift (Hall et al., 1991). It is important to emphasize that, in the absence of H diffusion, the primary inclusions should be underpressured during uplift and may tend toward higher densities (Fig. 9). Although the appearance of the inclusions may be qualitatively similar, in the latter case the lowest rather than highest density inclusions would most closely approximate the original isochore, and a negative rather than positive correlation between inclusion size and homogenization temperature should be observed. As previously mentioned, textures indicating internal underpressuring have been noted in primary fluid inclusions (Hall et al., 1991), but it is suggested that inclusions were initially underpressured and then reequilibrated to higher densities prior to the H diffusion event, which may have subsequently caused stretching. If the inclusions were to begin stretching during H diffusion, the effect would be to reduce the f_{H_2} in the inclusions by reducing the total pressure, perhaps resulting in further H diffusion to equilibrate f_{H_2}. This in turn would result in higher CH_4/CO_2 in the final inclusion fluid.

Values for δD of primary fluid inclusions

C, H, and O isotope analyses were collected from CH_4, H_2O, and CO_2 liberated from primary fluid inclusions in pyroxene (Hall et al., in preparation) (analyses by Isotope Specialists Inc.). Calculated bulk δD values for these inclusions range from −96 to −104 per mil SMOW. The δD values of the peak metamorphic (530 °C) fluid implied by the H isotope compositions of Ducktown biotite, muscovite, and chlorite analyzed by Addy and Ypma (1977) are −33 to −42 per mil, according to the fractionation factors of Suzuoki and Epstein (1976) and Graham et al. (1987). Furthermore, coexisting minerals give nearly identical δD_{H_2O} values, consistent with equilibration of H isotopes at peak metamorphic temperatures with little retrograde exchange.

Bulk δD values obtained from primary fluid inclusions are thus significantly lower than the estimated δD of H_2O in equilibrium with local hydrous phases during peak metamorphism. Because the fluid present in primary fluid inclusions was produced by local devolatilization reactions such as Equation 11, it should be in isotopic equilibrium with local hydrous minerals. Low δD primary fluid inclusions are consistent with the proposed H dif-

fusion model since molecular H diffusing into these inclusions would have very low δD values with respect to those of the aqueous grain boundary source fluids. Fractionation of H isotopes between H and H_2O in the source aqueous solution may have been as high as that for H_2 gas in equilibrium with H_2O vapor ($\Delta_{H_2O\text{-}H_2}$ = 360‰ at 450 °C, Bottinga, 1969). During diffusion, additional fractionation would result from the faster rate of diffusion of H relative to D; thus, the net fractionation between H reaching the inclusion and H_2O in the parent solution may have been significantly greater than $\Delta_{H_2O\text{-}H_2}$. Mass balance calculations using a $\Delta_{H_2O\text{-}H_2}$ of 360 per mil indicate that 16–18% of the H present in these inclusions would have to be added during diffusion. This value compares favorably with the calculated 12.5% necessary to effect the required compositional changes to the fluid inclusions.

Conclusions

Primary fluid inclusions in pyroxene, which formed at peak metamorphic conditions of 6 kbar and 550 °C with f_{O_2}-f_{S_2} values buffered near Py-Po-Mt, contain a normalized volatile composition of 93 mol% H_2O, 4 mol% CH_4, 3 mol% CO_2, and 0.1 mol% H_2S. Fluid speciation calculations and silicate mineral assemblages suggest that the trapped fluid should consist of 90 mol% H_2O, 10^{-7} mol% CH_4, 10 mol% CO_2, and 0.1 mol% H_2S. Methane was not a significant component of peak metamorphic fluids in ore zones.

Postentrapment speciation changes can account for the discrepancy in the CH_4/CO_2 ratio if the inclusions behaved as open systems and H diffused into the inclusions causing reduction of CO_2 to CH_4. This has been shown to be feasible if fluids in equilibrium with the bulk of the country rocks infiltrated the ore zones after peak metamorphism, because country rock fluids are buffered at f_{O_2} approximately 3 log units below oxidized portions of ore zones. If such an f_{H_2} gradient was established between inclusions and grain boundary fluids, diffusion of H into primary fluid inclusions may have occurred.

Values for δD of primary fluid inclusions are 65 per mil lower than equilibrium values at peak metamorphism. H diffusion would drastically lower the bulk δD of the inclusions by addition of isotopically light H. Mass balance calculations suggest that the amount of H necessary to lower δD will also result in sufficient compositional changes to reconcile calculated and observed fluid compositions. Hence, H diffusion is presently the best explanation for discrepancies between calculated and observed fluid compositions in primary fluid inclusions from Ducktown.

Acknowledgments

The authors gratefully acknowledge the Tennessee Chemical Company for permission to obtain and study samples from the Ducktown ore bodies. We thank mine geologist Charles Acker for his aid and helpful discussions, Bruce Nesbitt for lending us the thin section suite from his dissertation research, and Todd Solberg for help with electron microprobe analyses. Some of the computer programs used in this study were developed with the assistance of Bob Downs, John Doyle, and Mike Sterner. Additional discussions with Mike Sterner and Mathew Nyman were invaluable. Early reviews by Dave Hewitt, Don Rimstidt, and Dave Wesolowski are much appreciated. Insightful reviews by Terry Bowers and Bruce Nesbitt significantly improved the final presentation. This study was supported by grants from the Earth Sciences section of the National Science Foundation (NSF grant EAR-8618495), the American Chemical Society Petroleum Research Fund (grant 18861-G2), and by funds from the Department of the Interior's Mining and Mineral Resources Research Institute program administered by the Bureau of Mines under allotment grants G1164151, G1174151, and G1184151.

References cited

Addy, S.K. (1973) The problem of ore genesis at Ducktown, Tennessee. Interpretation of stable isotopes ($^{18}O/^{16}O$, $^{13}C/^{12}C$ and D/H), microprobe, and textural data. Ph.D. thesis, Columbia University, New York.

Addy, S.K., and Ypma, P.J.M. (1977) Origin of massive sulfide deposits at Ducktown, Tennessee: An oxygen, carbon, and hydrogen isotope study. Economic Geology, 72, 1245–1268.

Barton, P.B., and Skinner, B.J. (1979) Sulfide mineral stabilities. In H.L. Barnes, Ed., Geochemistry of hydrothermal ore deposits (2nd edition), p. 278–403. Wiley, New York.

Bottinga, Y. (1969) Calculated fractionation factors for carbon and hydrogen isotope exchange in the system calcite-carbon dioxide-graphite-methane-hydrogen-water vapor. Geochimica et Cosmochimica Acta, 33, 49–64.

Bowers, T.S., and Helgeson, H.C. (1983) Calculation of the thermodynamic and geochemical consequences of nonideal mixing in the system H_2O-CO_2-NaCl on phase relations in geologic systems: Metamorphic equilibria at high pressures and temperatures. American Mineralogist, 68, 1059–1075.

Brooker, D.D., Craig, J.R., and Rimstidt, J.D. (1987) Ore metamorphism and pyrite porphyroblast development at the Cherokee Mine, Ducktown, Tennessee. Economic Geology, 82, 72–86.

Burden, R.L., and Faires, J.D. (1985) Numerical analysis (3rd edition), 676 p. Prindle, Weber and Schmidt, Boston.

Burnham, C.W., and Wall, V.J. (1974) Fugacity coefficients for carbon dioxide in the range to 10 Kb, 1000 °C. Paper presented to NATO Conference "Volatiles in metamorphism, 1974."

Burnham, C.W., Holloway, J.R., and Davis, N.F. (1969) Thermodynamic properties of water to 1,000 °C and 10,000 bars. Geological Society of America Special Paper, 132, 96 p.

Cordier, P., Boulogne, B., and Doukhan, J. (1988) Water precipitation and diffusion in wet quartz and wet berlinite $AlPO_4$. Bulletin de Minéralogie, 111, 113–137.

Craig, J.R. (1983) Metamorphic features in Appalachian massive sulfides. Mineralogical Magazine, 47, 515–525.

Dubessy, J. (1984) Simulation des equilibres chimiques dans le systeme COH. Consequences methodologiques pour les inclusions fluides. Bulletin de Minéralogie, 107, 155–168.

Emmons, W.H., and Laney, F.B. (1926) Geology and ore deposits of the Ducktown mining district, Tennessee. U.S. Geological Survey Professional Paper, 139, 114 p.

Eugster, H.P., and Skippen, G.B. (1967) Igneous and metamorphic reactions involving gas equilibria. In P.H. Abelson, Ed., Researches in geochemistry, vol. 2, p. 492–520. Wiley, New York.

Ferry, J.M., and Baumgartner, L. (1987) Thermodynamic models of molecular fluids at the elevated pressures and temperatures of crustal metamorphism. In Mineralogical Society of America Reviews in Mineralogy, 17, 323–366.

Flowers, G.C., and Helgeson, H.C. (1983) Equilibrium and mass transfer during progressive metamorphism of siliceous dolomites. American Journal of Science, 283, 230–286.

French, B.M. (1966) Some geological implications of equilibrium between graphite and a C-H-O gas phase at high temperatures and pressures. Reviews of Geophysics, 4, 223–253.

Gair, J.E., and Slack, J.F. (1984) Deformation, geochemistry, and origin of massive sulfide deposits, Gossan Lead District, Virginia. Economic Geology, 79, 1483–1520.

Graham, C.M., Viglino, J.A., and Harmon, R.S. (1987) Experimental

study of hydrogen-isotope exchange between aluminous chlorite and water and of hydrogen diffusion in chlorite. American Mineralogist, 72, 566–579.

Hadley, J.B., and Goldsmith, R. (1963) Geology of the eastern Great Smokey Mountains, North Carolina and Tennessee: U.S. Geological Survey Professional Paper, 349-B, 118 p.

Hall, D.L., and Bodnar, R.J. (1989) Methane in fluid inclusions from granulites: A product of hydrogen diffusion? Geochimica et Cosmochimica Acta, 54, 641–651.

Hall, D.L., Sterner, S.M., and Bodnar, R.J. (1989a) Fluid inclusions in regional metamorphic rocks: Experimental evidence for post-entrapment volumetric and compositional modifications (abs.). Tenth European current research on fluid inclusions, p. 44. Royal School of Mines, Imperial College, University of London, London, United Kingdom.

——— (1989b) Experimental evidence for hydrogen diffusion into fluid inclusions in quartz. Geological Society of America Abstracts with Programs, 21, A-358.

Hall, D.L., Bodnar, R.J., and Craig, J.R. (1991) Fluid inclusion constraints on the uplift history of the metamorphosed massive sulfide deposits at Ducktown, Tennessee. Journal of Metamorphic Geology, in press.

Harting, P., and Maass, I. (1980) Neue Ergebnisse zum Kohlenstoff-Isotopenaustausch im System CH_4-CO_2. Mitteilungen zur 2. Arbeitstagung "Isotope in der Natur," vol. 2b, p. 13–24. Zentralinstitut für Isotopen- und Strahlenforschung, Leipzig, Germany.

Hatcher, R.D., Jr. (1978) Tectonics of the western Piedmont and Blue Ridge, Southern Appalachians: Review and speculations. American Journal of Science, 278, 276–304.

Henry, D.K., Craig, J.R., and Gilbert, M.C. (1979) Ore mineralogy of the Great Gossan Lead, Virginia. Economic Geology, 74, 645–656.

Hewitt, D.A. (1973) Stability of the assemblage muscovite-calcite-quartz. American Mineralogist, 58, 785–791.

Holcombe, R.J. (1973) Mesoscopic and microscopic analysis of deformation and metamorphism near Ducktown, Tennessee, 225 p. Unpublished Ph.D. thesis, Stanford University, Stanford, California.

Holloway, J.R. (1977) Fugacity and activity of molecular species in supercritical fluids. In D.G. Fraser, Ed., Thermodynamics in geology, p. 161–181. Reidel, Dordrecht, The Netherlands.

——— (1981) Compositions and volumes of supercritical fluids in the earth's crust. In L.S. Hollister and M.L. Crawford, Eds., Short course in fluid inclusions: Applications to petrology, p. 13–38. Mineralogical Association of Canada, Calgary.

Hunt, J.A., and Kerrick, D.M. (1977) The stability of sphene; experimental redetermination and geologic implications. Geochimica et Cosmochimica Acta, 41, 279–288.

Jacobs, G.K., and Kerrick, D.M. (1981) Devolatilization equilibria in H_2O-CO_2 and H_2O-CO_2-NaCl fluids: An experimental and thermodynamic evaluation at elevated pressures and temperatures. American Mineralogist, 66, 1135–1153.

Johannes, W., and Orville, P.M. (1972) Zur Stabilitat der mineralparagenesen Muskovit + Calcit + Quarz, Zoisit + Muskovit + Quarz, Anorthit + K-feldspat, und Anorthit + Calcit. Fortschritte der Mineralogie, 50, 46–47.

Kats, A. (1962) Hydrogen in alpha-quartz. Philips Research Report, 17, 1–31, 133–279.

Kats, A., Haren, Y., and Stevels, J.M. (1962) Hydroxyl groups in β-quartz. Physical Chemistry of Glasses, 3, 69–75.

Kronenberg, A.K., Kirby, S.H., Aines, R.D., and Rossman, G.R. (1986) Solubility and diffusional uptake of hydrogen in quartz at high water pressures: Implications for hydrolytic weakening. Journal of Geophysical Research, 91, 12723–12744.

Magee, M. (1968) Geology and ore deposits of the Ducktown district, Tennessee. In J.D. Ridge, Ed., Ore deposits of the United States: 1933–1967, p. 207–241. American Institute of Mining, Metallurgy, and Petroleum Engineering, Inc., New York.

Mauger, R.L. (1972) A sulfur isotope study of the Ducktown Tennessee District, U.S.A. Economic Geology, 67, 497–510.

Nesbitt, B.E. (1979) Regional metamorphism of the Ducktown, Tennessee massive sulfides and adjoining portions of the Blue Ridge Province, 216 p. Unpublished Ph.D. thesis, University of Michigan, Ann Arbor, Michigan.

——— (1982) Metamorphic sulfide-silicate equilibria in the massive sulfide deposits at Ducktown, Tennessee. Economic Geology, 77, 364–378.

Nesbitt, B.E., and Essene, E.J. (1982) Metamorphic thermometry and barometry of a portion of the southern Blue Ridge province. American Journal of Science, 282, 701–729.

Nesbitt, B.E., and Kelly, W.C. (1980) Metamorphic zonation of sulfides, oxides and graphite in and around the orebodies at Ducktown, Tennessee. Economic Geology, 75, 1010–1021.

Ohmoto, H., and Kerrick, D. (1977) Devolatilization equilibria in graphitic systems. American Journal of Science, 277, 1013–1044.

Pasteris, J.D., and Wanamaker, B.J. (1988) Laser Raman microprobe analysis of experimentally re-equilibrated fluid inclusions in olivine: Some implications for mantle fluids. American Mineralogist, 73, 1074–1088.

Robie, R.A., Hemingway, B.S., and Fisher, J.R. (1978) Thermodynamic properties of minerals and related substances at 298.15 K and 1 bar (10^5 Pascals) pressure and at higher temperatures. U.S. Geological Survey Bulletin 1452, 456 p.

Roedder, E. (1981) Origin of fluid inclusions and changes that occur after trapping. In L.S. Hollister and M.L. Crawford, Eds., Short course in fluid inclusions: Applications to petrology, p. 103–137. Mineralogical Association of Canada, Calgary.

Roedder, E., and Skinner, B.J. (1968) Experimental evidence that fluid inclusions do not leak. Economic Geology, 63, 715–730.

Ryzhenko, B.N., and Volkov, V.P. (1971) Fugacity coefficients of some gases in a broad range of temperatures and pressures. Geochemistry International, 8, 468–481.

Sackett, W.M., and Chung, H.M. (1979) Experimental confirmation of the lack of carbon isotope exchange between methane and carbon oxides at high temperatures. Geochimica et Cosmochimica Acta, 43, 273–276.

Shaw, H.R., and Wones, D.R. (1964) Fugacity coefficients for hydrogen gas between 0°–1000 °C for pressures to 3000 atm. American Journal of Science, 262, 918–929.

Slaughter, J., Kerrick, D.M., and Wall, V.J. (1975) Experimental and thermodynamic study of equilibria in the system CaO-MgO-SiO_2-H_2O-CO_2. American Journal of Science, 275, 143–162.

Sterner, S.M., and Bodnar, R.J. (1989) Synthetic fluid inclusions—VII. Re-equilibration of fluid inclusions in quartz during laboratory-simulated burial and uplift. Journal of Metamorphic Geology, 7, 243–260.

Sterner, S.M., Hall, D.L., and Bodnar, R.J. (1988) Post-entrapment compositional changes in fluid inclusions: Experimental evidence for water diffusion in quartz. Geological Society of America Abstracts with Programs, 20, A100.

Suzuoki, T., and Epstein, S. (1976) Hydrogen isotope fractionation between OH-bearing minerals and water. Geochimica et Cosmochimica Acta, 40, 1229–1240.

Toulmin, P., III, and Barton, P.B. (1964) A thermodynamic study of pyrite and pyrrhotite. Geochimica et Cosmochimica Acta, 28, 641–671.

White, S. (1973) Dislocations and bubbles in vein quartz. Nature, 243, 11–14.

Wilkins, R.W.T., and Barkas, J.P. (1978) Fluid inclusions, deformation and recrystallization in granite tectonites. Contributions to Mineralogy and Petrology, 65, 293–299.

Ziegenbein, D., and Johannes, N. (1980) Graphite in C-H-O fluids: An unsuitable compound to buffer fluid composition at temperatures up to 700 °C. Neues Jahrbuch für Mineralogie Monatshefte, 7, 289–305.

Manuscript received December 15, 1989
Manuscript accepted April 16, 1991